ASSESSMENT OF COMBINED DROUGHT INDEX (CDI) FOR DROUGHT MONITORING IN THE PHILIPPINES DURING THE 2018-2019 EL NIÑO

Michael Angelo Valete[1,2], Paul Daniel Ang[1,2], Archie Veloria[2], Gay Jane Perez[1,2]
[1]Institute of Environmental Science and Meteorology, University of the Philippines Diliman, Quezon City 1101, Metro Manila, Philippines
Email: michael.valete@philsa.gov.ph, danna.ang@philsa.gov.ph
[2]Philippine Space Agency (PhilSA), University Laboratory for Small Satellites and Space Engineering Systems (ULyS3ES) Building, University of the Philippines Diliman, Quezon City 1101, Metro Manila, Philippines
Email: archie.veloria@philsa.gov.ph, gay.perez@philsa.gov.ph

KEY WORDS: agricultural drought, crop production loss, ENSO

ABSTRACT: The Philippines is vulnerable to the impacts drought, which resulted to millions of dollars of damages in crops and livestock. In this study, a combined drought index (CDI) was developed to monitor the transition from meteorological to agricultural drought. It combines monthly land surface temperature (LST), normalized difference vegetation index (NDVI), and the three-month rainfall represented by the standardized precipitation index (SPI-3). The CDI has four levels of increasing severity, *Watch*, *Warning*, *Alert-1*, and *Alert-2*, where *Watch* indicates significant precipitation deficit and *Alert-2* indicates significant anomalies of the three input variables. The performance of CDI was evaluated using provincial crop production loss reports during the 2018-2019 El Niño and was also compared with SPI-3 and the Vegetation Health Index (VHI). Consistent CDI levels were observed from October to December 2018 affecting 43% to 51% of the provinces of the country. The drought peak in terms of level and percentage of affected provinces identified by CDI occurred in March and April 2019 when *Alert-2* was observed and at least 75% of the provinces exhibited drought signals. CDI outperformed SPI-3 and VHI in terms of accuracy (precision) being 67% (67%) compared to 62% (61%) and 57% (66%) of SPI-3 and VHI, respectively. However, while the CDI has a high hit rate of 85%, it also has a high false alarm rate of 59%. Overall, this study demonstrates how the CDI can be a viable metric that can be used by stakeholders for early warning systems of drought in the country.

1. INTRODUCTION

Drought is a complex and naturally occurring phenomenon that can inflict adverse impacts on agriculture, economy, and society all over the world (Dai, 2011). It is widely considered as a slow-onset event caused by a lack of precipitation for an extended period. Drought can be categorized based on its types: meteorological, agricultural, hydrological, and socioeconomic (Wilhite and Glantz 1985; Dai, 2011). Meteorological drought begins with a precipitation deficit for several months. The persistence of such an event paired with other stressors such as increase in temperature and evapotranspiration may affect soil moisture levels, affecting the quality and quantity of crop yields. The phenomenon is then called agricultural drought. Hydrological drought occurs once lower water levels in lakes and reservoirs, low streamflow in rivers, and reduced groundwater start to manifest (Van Loon, 2015). The effect of these droughts on societies is the socioeconomic drought.

Several drought indices have been developed to examine the characteristics of drought in terms of its intensity, onset, and termination. The standardized precipitation index (SPI), a rainfall-based index, is the recommended index by the World Meteorological Organization (WMO) for monitoring meteorological drought (Hayes et al., 2011). The use of several accumulations of precipitation in SPI (SPI timescales) allows the monitoring of different drought types. For example, Gumus and Aglin (2017) examined meteorological and hydrological drought characteristics in Ceyhan River Basins, Turkey using 3-month, 6-month, and 12-month SPI timescales. Kogan (1995) developed the Vegetation Health Index (VHI) to monitor agricultural drought globally. VHI is a satellite-based drought index derived from the Temperature Condition Index (TCI) and the Vegetation Condition Index (VCI) and has been found effective in monitoring agricultural drought impacts (Kogan et al., 2012; Kogan, 1995; Bento et al., 2018). VHI utilizes the inverse relationship found between Land Surface Temperature (LST) and the Normalized Difference Vegetation Index (NDVI) where high NDVI and low LST indicate dense vegetation while low NDVI paired with high LST vegetation show heat stress (Bento et al., 2018).

In recent years, researchers began to develop Combined Drought Indices (CDIs) based on the combination of multiple drought indicators and indices for drought monitoring and early warning. The CDI developed by Sepulcre-Cantro et al. (2012) was conceptualized based on the cause-and-effect relationship between drought parameters such as rainfall through SPI, soil moisture, and the fraction of photosynthetically active radiation

(fAPAR). The consistent lack of rainfall will eventually lead to a soil moisture deficit that will affect the crops. This CDI is the current drought monitoring tool used by the European Drought Observatory (EDO). A similar approach was made by Balint et al. (2013) in early warning of drought in Kenya with inputs being rainfall, temperature, and vegetation condition.

In the Philippines, drought events over the past decades have impacted the agricultural sector. Most of these events are caused by the warm phase of the El Niño-Southern Oscillation (hereinafter referred to as El Niño) which brings drier conditions throughout the country (Hilario et al., 2009). For example, the strong 2015-2016 episode devastated agriculture and the economy with USD 327 million worth of crop damages (Sutton et al., 2019) while the recent 2018-2019 weak episode caused USD 157 million worth of crop damages (NDRRMC, 2019). Drought in the country is being monitored by Philippine Atmospheric, Geophysical and Astronomical Services Administration (PAGASA) which uses station-based rainfall indices such as Percent Normal Precipitation (PNP) and SPI. Station-based monitoring only covers the surrounding areas hence requires a dense network of stations to cover an entire country. Additionally, SPI and PNP are both precipitation-based indices and are best for monitoring meteorological drought. Perez et al. (2016) developed the localized agricultural drought index called Standardized Vegetation Temperature Index (SVTR) from LST and NDVI. Similar to VHI, SVTR utilizes the inverse relationship of NDVI and LST and was able to detect below-normal rice yields in the country during the 2015-2016 El Niño-driven drought. In addition, Perez et al. (2022) highlighted the importance of using multiple satellite-derived drought indices and indicators in characterizing the nationwide drought development caused by the recent 2018-2019 El Nino.

This research aims to develop a satellite-derived CDI that uses rainfall, temperature, and vegetation information to monitor the evolution from meteorological to agricultural drought. The performance of the CDI is tested using provincial rice and corn damage reports due to the recent 2018-2019 weak El Niño. The proposed index aims to help decision-makers in early warning of drought to mitigate its impacts.

2. METHODOLOGY

2.1. Data

2.1.1 Remotely sensed data: In this study, satellite-based data from June 2000 to December 2019 were used to derive CDI. The monthly rainfall data used was the Integrated Multi-Satellite Retrievals for Global Precipitation Measurement (GPM IMERG) final run version 6. This rainfall dataset was developed by the United States GPM team with an algorithm involving a combination of rainfall measurements from the GPM constellation of satellites and geostationary satellites, and merging with observations from the ground (Huffman et al., 2020). The IMERG final run version 6, with a 0.1° × 0.1° resolution, was downloaded from the National Aeronautics and Space Administration (NASA) website (https://gpm.nasa.gov/) and was clipped to focus on the landmass of the Philippines. Meanwhile, the monthly NDVI and LST data were acquired from the Moderate Resolution Imaging Spectroradiometer (MODIS) onboard the Terra satellite. These datasets were readily available online in HDF format that can be accessed from Land Processes Distributed Active Archive Center (LP DAAC) Data Pool (https://lpdaac.usgs.gov/). The MOD13C2 and MOD11C3 version 6 provide the monthly pixelwise values at 0.05° × 0.05° resolution of NDVI and LST, respectively.

2.1.2 Drought damage reports: The provincial rice and corn damage reports due to the effect of El Niño were acquired from Situation Report No. 21 of the National Disaster Risk Reduction and Management Council (NDRRMC, 2019). These damage reports are the official records of the Department of Agriculture (DA) as of April 2019. Included in this situation report are the total cost of damage to rice and corn, the number of the affected populations, and municipalities that declared a state of calamity.

2.1.3 Oceanic Niño Index: The Oceanic Niño Index (ONI) was used to identify the development of El Niño, from its onset until its termination. ONI is the three-month running mean of sea surface temperature (SST) anomalies in the Niño-3.4 region, along the eastern-central equatorial Pacific Ocean between 5 °S - 5 °N latitude and 120 °W - 170 °W longitude. An El Niño event is considered when ONI reaches 0.5 °C for five (5) consecutive months. The ONI from 2018 to 2019 was downloaded from the National Oceanic and Atmospheric Administration - Climate Prediction Center (NOAA CPC) website (https://www.cpc.ncep.noaa.gov/).

The weak El Niño of 2018-2019 began with an increase in ONI (Figure 1). In October 2018, ONI reached 0.8 °C and was consistent to be above 0.5 °C until June 2019. The ONI value then dropped to 0.3 °C the following month which depicts the termination of El Niño.

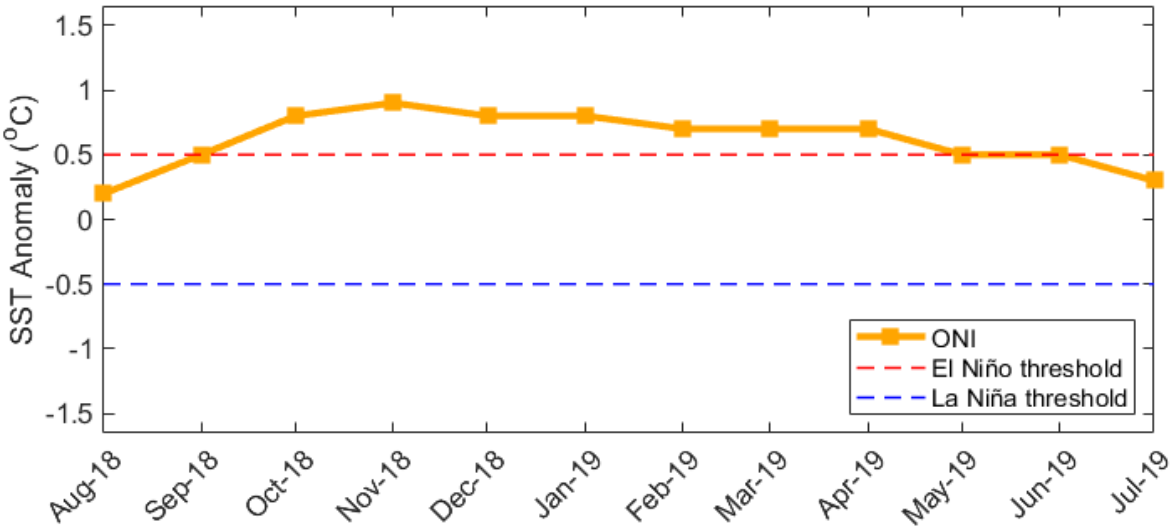

Figure 1. Oceanic Niño Index from August 2018 to July 2019.

2.2. Inputs and derivation of CDI

2.2.1 Standardization of CDI inputs: SPI is utilized around the world for monitoring drought. It is based on the deviation of rainfall from its long-term mean, preferably 30 years or more. The strength of SPI allows for different SPI timescales (1-month, 3-month, 12-month, etc.), allowing the monitoring of short-term and long-term precipitation deficits that may affect agriculture and hydrology (Hao & AghaKouchak, 2013). SPI also identified droughts in the United States earlier than the other indices (Mo, 2011); hence it is suitable for drought onset identification.

Twenty (20) years of monthly GPM rainfall data were used to derive SPI. To match the resolution of MODIS NDVI and LST, the rainfall dataset was regridded to 0.05° × 0.05° using linear interpolation. The 3-month SPI timescale (hereinafter referred to as SPI-3) was chosen as it is related to short-term drought soil moisture stress (Ji & Peters, 2003; Mlenga et al., 2019). Calculation of SPI-3 involves fitting the 3-month precipitation total to the gamma function. The probability density function was then transformed to a Gaussian distribution which gives the SPI value. In this case, an SPI value is the number of standard deviations from which the observed 3-month precipitation deviates from its long-term mean. Detailed calculations of SPI can be found in the literature (Gumus and Aglin, 2017). A negative SPI value denotes dry conditions while positive values indicate wet conditions.

For the temperature and vegetation information of CDI, the standardized LST and NDVI (stdz_LST and stdz_NDVI, respectively) from MODIS were calculated using:

$$z_i = \frac{x_i - u}{\sigma} \qquad \text{Equation (1)}$$

where z_i refers to the standardized value of NDVI (or LST) for month i, x_i is the NDVI (or LST) for the month i, while u and σ are the mean and standard deviation of all NDVI (or LST) occurring in the same calendar month as month i, respectively.

2.2.2 Combined Drought Index (CDI): The Combined Drought Index (CDI) developed in this study had 0.05° × 0.05° resolution and was based on the satellite-derived parameters of GPM rainfall, along with MODIS LST and NDVI. Specifically, the SPI-3, stdz_LST, and stdz_NDVI were used as inputs of CDI which consist of present atmospheric, land, and vegetative conditions necessary for agricultural drought monitoring. Trigger thresholds for both SPI-3 and stdz_NDVI are set to ≤ -1.0 while ≥ 1.0 for stdz_LST. CDI has four (4) levels of increasing severity (shown in Figure 2). The Watch stage occurs once there is a significant precipitation deficit as observed from SPI-3 and proceeds to the Warning stage when paired with a consequential increase in temperature. Alert-1 starts when vegetation health decreases combined with notable anomalies in either precipitation or temperature. Alert-2 occurs when all three indices hit the trigger threshold for the current month.

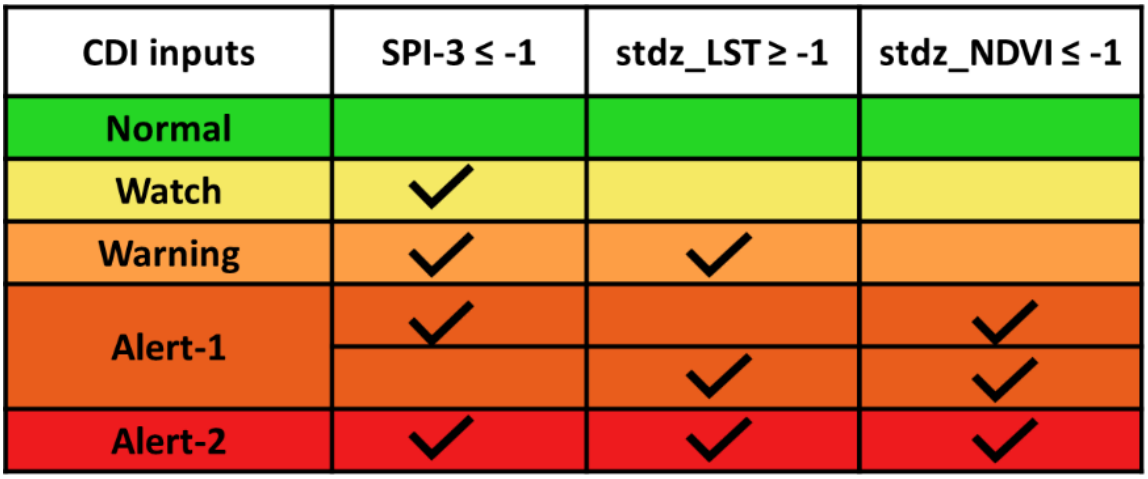

Figure 2. Color-coded CDI signal classification.

2.3 Evaluation of the performance of CDI using drought damage reports

The provincial drought damage reports of the Department of Agriculture (DA) obtained from the NDRRMC 2019 report (see Section A.2.) were used to assess the performance of CDI. For CDI, a drought event is defined as a period with consistent CDI signals for at least 2 months containing either Alert-1 or Alert-2 or at least 3 months with Watch and/or Warning signals. Provinces with recorded damage to rice and/or corn are considered drought affected. With these definitions, a confusion matrix for the assessment of the performance of CDI was calculated. The confusion matrix includes the true positive (TP), false positive (FP), true negative (TN), and false negative (FN) rates. TP and TN are the actual drought and non-drought affected provinces correctly identified by CDI, respectively. FP and FN correspond to those that are incorrectly identified as drought and non-drought, respectively. After calculating the values in the confusion matrix, the performance metrics were then calculated. Table 1 shows the equations used in calculating the metrics. Accuracy describes how CDI correctly identifies drought and non-drought-affected provinces while precision is the probability that the CDI detects drought. Hit rate signifies how frequently CDI correctly detects drought, while false alarm rate implies how frequently the index misidentified non-drought affected provinces as drought affected. Miss rate is how frequently CDI misses drought occurrences in a province while the true negative rate indicates how frequently CDI correctly identifies non-drought events in a province. A similar analysis was done on SPI-3 and VHI to compare with the performance of CDI. Detailed calculation of VHI can be found in the study of Bento et al. (2018).

Table 1. The equation of the performance metrics derived from the confusion matrix.

Performance Metric	Equation
Accuracy	$\frac{TP+TN}{\sum Number\ of\ samples}$
Precision	$\frac{TP}{TP+FP}$
Hit rate	$\frac{TP}{TP+FN}$
False alarm rate	$\frac{FP}{TP+FP}$
Miss rate	$\frac{FN}{FN+TP}$
True negative rate	$\frac{TN}{TN+FP}$

3. RESULT AND DISCUSSION

3.1 Drought development as seen by CDI

The onset of the weak El Niño in 2018-2019 begins with the ONI reaching the 0.5 °C threshold in September 2018. The phenomenon peaked around November 2018 and continued until June 2019 when the ONI decreased to 0.3 °C the following month which depicts its termination. The spatiotemporal development of drought as seen by CDI is shown in Figure 3 while the percentage of provinces with CDI signals is shown in Figure 4. Also included in Figure 4 is the development (from onset to termination) of the El Niño event.

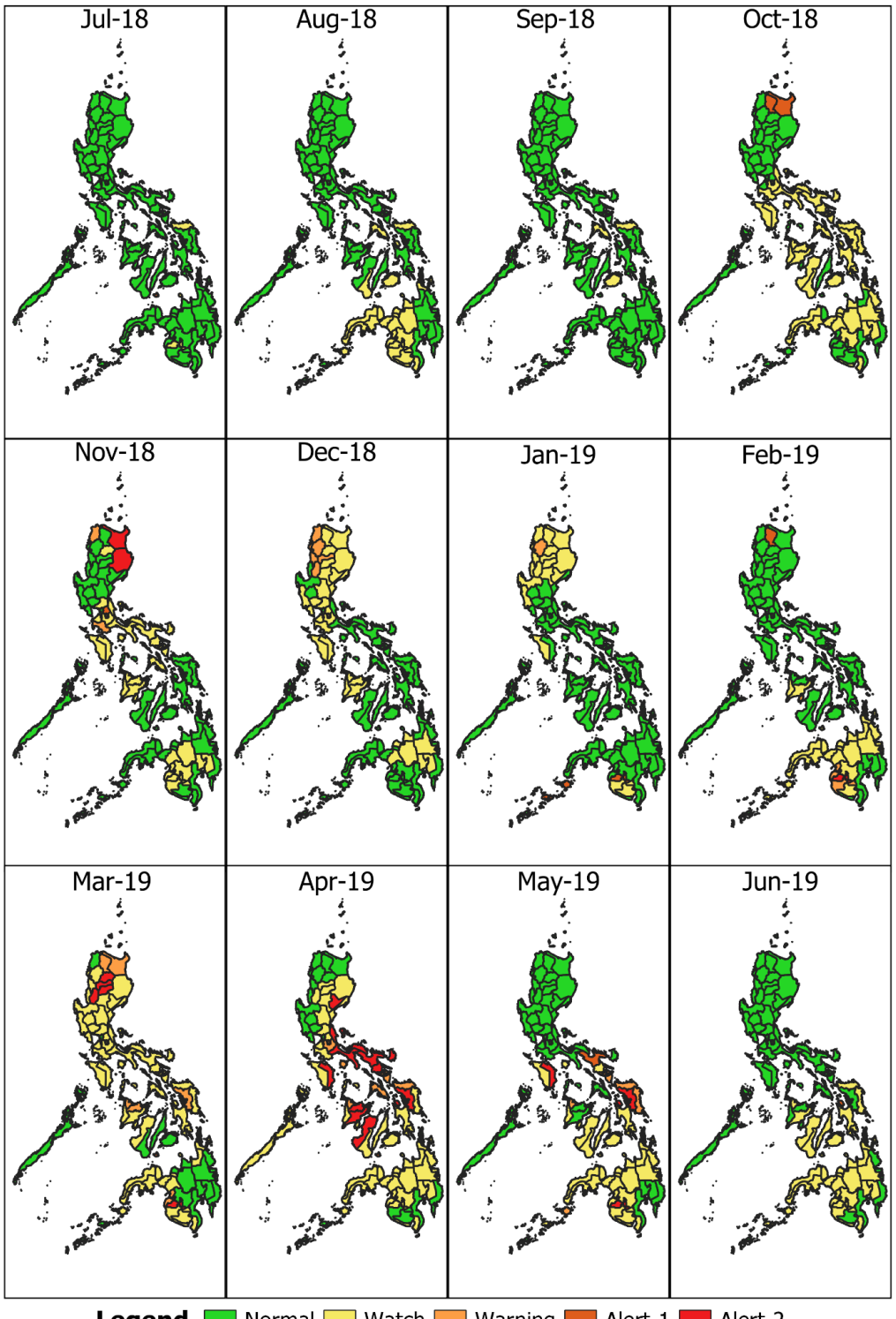

Figure 3. Monthly Combined Drought Index (CDI) maps from July 2018 to June 2019.

In September 2018, at the onset of El Niño, only three (3) provinces had Watch signals suggesting precipitation deficit. Consistent CDI signals were observed in 43% to 51% of the provinces from October to December 2018. During these months, signals are mostly Watch still suggesting a consistent precipitation deficit. Alert-1 to Alert-2 signals were also observed in northern provinces of the Philippines which indicate anomalies in the rainfall, temperature, and vegetation health. These are also the months in which crops are being harvested/planted for the main/second cropping season (FAO, 2016). The number of affected provinces decreased to 26% and 31% in January and February 2019 with signals mostly Watch. While we expected the development of drought from Watch to Alert-1 and/or Alert-2, in some provinces, such as Cagayan, Isabela, and Apayao, CDI recorded stronger signals than Watch at the beginning of the event. Future studies to improve the characterization of the development of drought will be done.

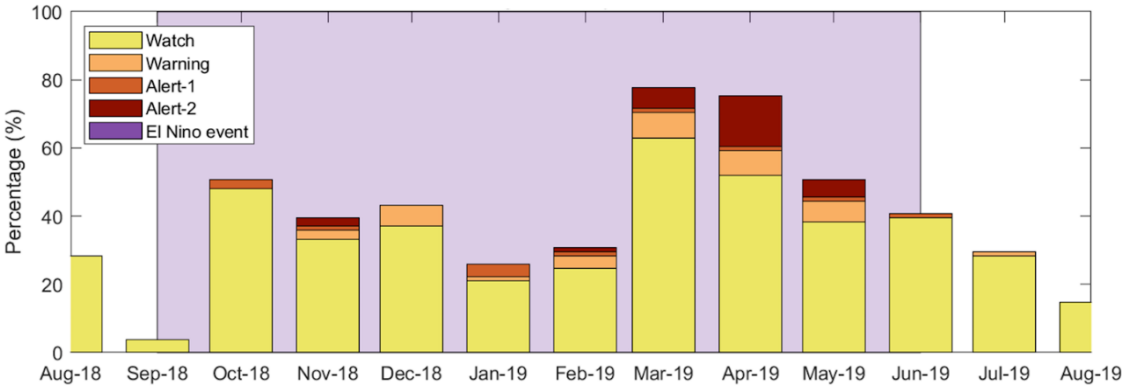

Figure 4. Monthly percentage of CDI drought levels across provinces during the 2018-2019 El Niño.

The peak of drought events in terms of CDI signals and the percentage of affected provinces based on CDI was observed during March and April 2019. During these months, at least 75% of the provinces had exhibited CDI signals ranging from Watch to Alert-2. This means that the effect of persistent precipitation deficit had already affected the crops. Moreover, drought occurrences during these months are critical as these are the typical dry months in most parts of the country in which crops are already at the harvesting stage. Thus, lower-than-normal temperatures brought by El Niño could cause significant damage to crops. The number of provinces with CDI signals started to decrease in June 2019 with 40% of the provinces experiencing mostly precipitation deficit (Watch) until it was 30% and 15% in July and August, respectively. This shows that the effect of El Niño on seasonal precipitation was felt even after its termination. The performance of CDI when compared to the provincial crop production loss of rice and corn is presented in the next section.

3.2 Investigation of the performance of CDI during the 2018-2019 El Niño event

The weak El Niño of 2018-2019 caused agricultural damage to rice and corn in most of the provinces of the country. Monetary damages from this event per province ranged from a hundred thousand pesos to PHP 1.2 billion. Provinces in the northeastern part of the country had the highest incurred damage with at least PHP 900 million (Figure 5a). From Figure 3, a series of Watch, Warning, Alert-1, and Alert-2 were observed in these areas starting October 2018 to April 2019 suggesting a significant reduction in rainfall and vegetation health, and an increase in temperature. This would have affected the crops as seen in the crop damage reports.

Figure 5b shows the number of drought events as identified by CDI. Some provinces in the central-western Philippines and in Mindanao had two drought events. This is possibly due to the above-normal rainfall in between the drought events that caused the short breaks. Provinces in Central Luzon had no identified CDI drought events and only the province of Bulacan had recorded crop damage. Coincidentally, provinces in Central Luzon were the largest rice producers in the country. This can be attributed to a better irrigation system set up in these areas. Validation of this reason will be pursued in future studies.

A side-by-side comparison between Figure 5a and Figure 5b reveals that provinces with recorded damages have corresponding CDI drought events. This shows the capability of CDI in identifying drought impacts on the ground. On the other hand, CDI also identified drought and non-drought events in provinces without and with recorded drought damages, respectively. This was seen in some provinces in western Luzon, central Visayas, and northern Mindanao. A summary of the spatial comparison between the two figures is shown in Figure 5c. The inclusion of more drought events and the El Niño phenomenon in the analysis will be done in the future to calibrate the threshold of CDI and improve its performance.

The comparison of the performance of CDI with VHI and SPI-3, two established drought indices, in detecting drought impacts is shown in Table 2. Overall, better performance was observed in CDI compared to VHI and SPI with high accuracy (precision) of 67% (67%) for CDI against 62% (61%) and 57% (66%) of SPI-3 and VHI, respectively. The high hit rate (85%) and low miss rate (15%) of CDI suggest the viability of CDI in detecting drought impacts. On the contrary, CDI overidentified drought events as seen in the high false alarm rate (59%) and fairly low true negative rate (41%).

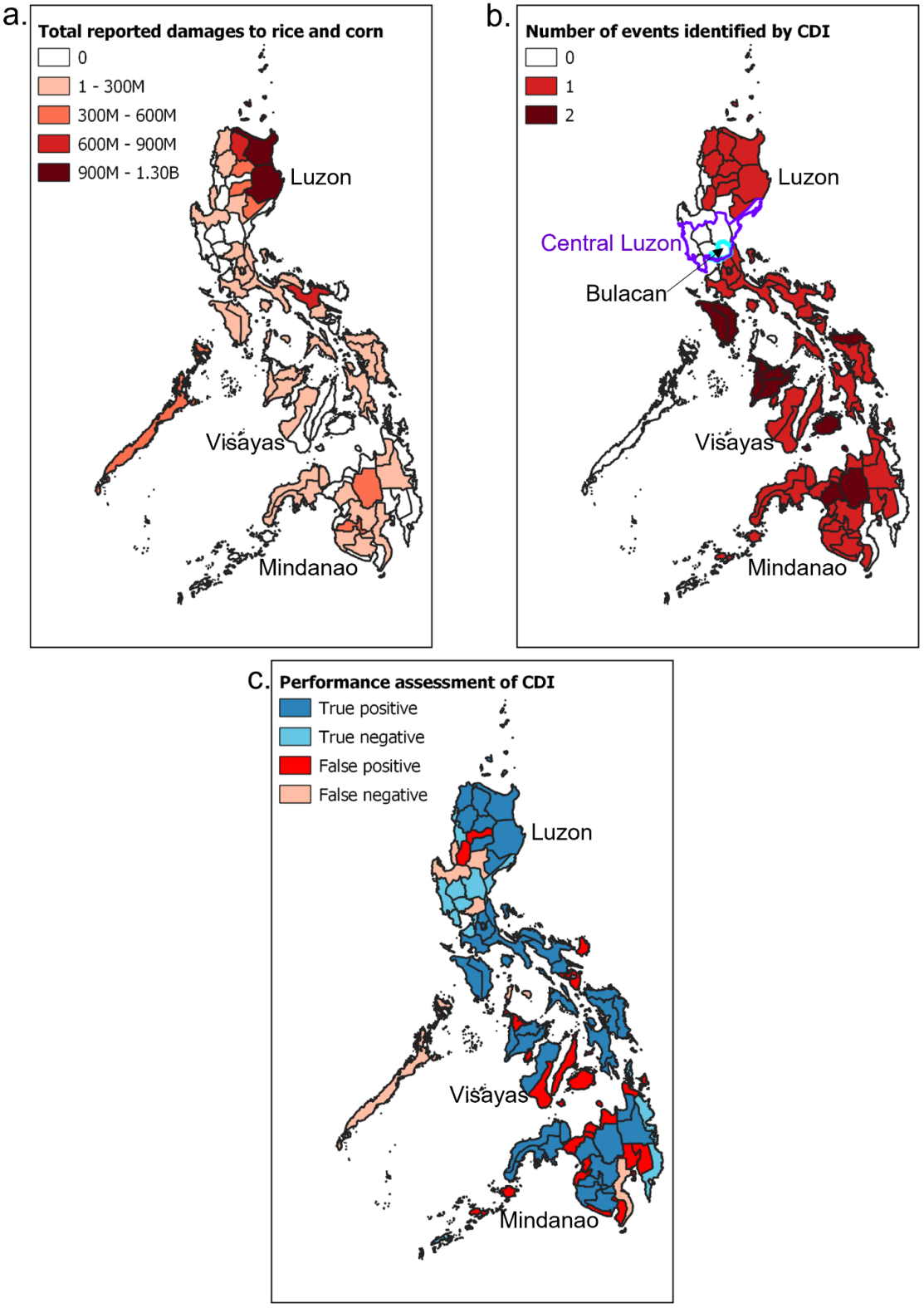

Figure 5. (a) Total reported damages to rice and corn during the weak El Niño of 2018-2019, (b) number of events identified by CDI, and (c) performance assessment of CDI when compared to drought damage reports.

SPI-3, the rainfall-based index, had the highest possible hit rate of 100% but also had a high false alarm rate (91%). This is because SPI-3 can identify drought impacts but would also be able to identify meteorological droughts that do not propagate to agricultural drought. This is shown in Figure 6a where all of the provinces with impacts are captured by SPI but also detected drought in unaffected provinces. In this context, SPI-3 is better at identifying the onset of drought events that may or may not propagate to agricultural drought.

Table 2. Summary of Performance of CDI, SPI-3, and VHI.

Performance scores (%)	CDI	SPI-3	VHI
Accuracy	67	62	57
Precision	67	61	66
Hit Rate	85	100	54
Miss Rate	15	0	46
False Alarm Rate	59	91	38
True negative Rate	41	9	62

The drought impacts of the 2018-2019 El Niño were not fully captured by VHI as evident in the low hit (54%) and high miss rates (46%). Additionally, VHI's hit and miss rates were the worst among the three indices. VHI got the lowest false alarm (38%) and highest true negative (62%) rate. Assessment of the comparison with VHI and provinces with actual impacts (Figure 6b) revealed that VHI could not capture drought impacts on most provinces in Mindanao. Additionally, VHI identified drought in some provinces in central Luzon but no actual damage has been recorded. One possible explanation for VHI having low hit rates is that there were some drought impacts that were due to an extended period of below normal rainfall and had affected the crops (combination of Watch and Alert-1) but had no significant increase in temperature thereby the misidentification. While VHI is a well-known satellite-based agricultural drought index, additional information on parameters such as rainfall is extremely important to fully understand the phenomenon for monitoring drought and its development.

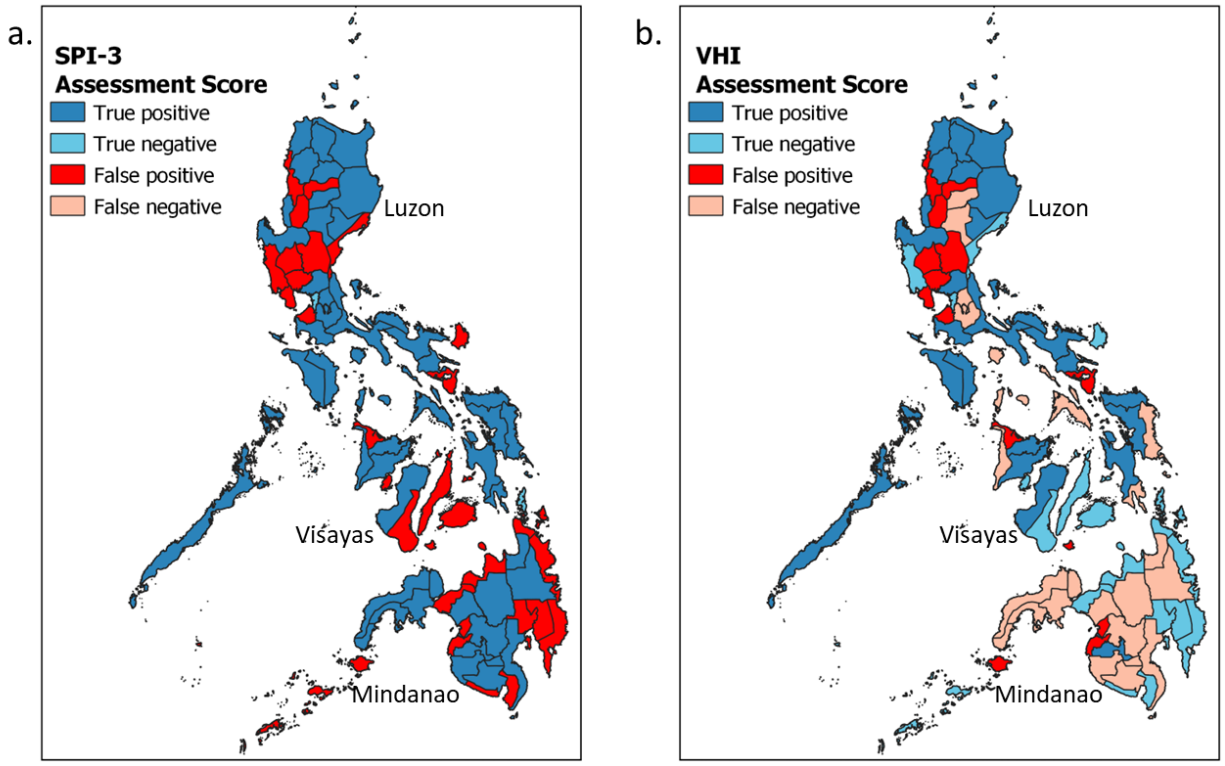

Figure 6. Performance assessment of (a) SPI and (b) VHI when compared to drought damage reports.

4. CONCLUSION

This study presents a satellite-based drought index based on the combination of the standardized anomalies of rainfall, LST, and NDVI. The developed CDI has four drought signals (Watch, Warning, Alert-1, and Alert-2) which follow the transition from meteorological (Watch and Warning) to agricultural drought (Alert-1 and Alert-2). CDI was evaluated with the recent 2018-2019 weak El Niño. The performance of CDI was also assessed using the drought damages in rice and corn brought by El Niño and was compared with SPI-3 and VHI. In most provinces, the spatial development of drought was characterized by CDI. The peak of the event in terms of the percentage of affected provinces as identified by CDI occurred in March and April when at least 75% were affected. In the evaluation of the performance of CDI, SPI-3, and VHI with the drought damages due to El Niño, CDI outperformed the two suggesting its capability in detecting drought and its impacts. While CDI had the highest accuracy and precision (both 67%), it also had a high false alarm rate (59%). Future studies will involve the calibration of CDI signals using other drought events to improve the characterization of these events. Overall, this study demonstrates the potential of CDI in monitoring drought for early detection and mitigation.

5. ACKNOWLEDGEMENT

This research was supported by the Drought and Crop Assessment and Forecasting Phase 2 (DCAF2) project funded by the Department of Science and Technology - Philippine Council for Agriculture, Aquaculture and Natural Resources Research and Development (DOST-PCAARRD) and the Satellite Mission Analysis, Planning, Product Enhancement and Development (SatMAPPED) project of the Philippine Space Agency (PhilSA).

6. REFERENCES

Balint, Z., Mutua, F., Muchiri, P., & Omuto, C. T., 2013. Monitoring drought with the combined drought index in Kenya. In Developments in earth surface processes (Vol. 16, pp. 341-356). Elsevier.

Bento, V. A., Gouveia, C. M., DaCamara, C. C., & Trigo, I. F., 2018. A climatological assessment of drought impact on vegetation health index. Agricultural and Forest Meteorology, 259, 286-295.

Dai, A., 2011. Drought under global warming: A review. Wiley Interdisciplinary Reviews: Climate Change, 2(1), 45-65.

Food and Agricultural Organization, 2016. Global Information and Early Warning System (GIEWS) Update - The Philippines. Taken from https://www.fao.org/3/i6375e/i6375e.pdf

Gumus, V., & Algin, H. M., 2017. Meteorological and hydrological drought analysis of the Seyhan−Ceyhan River Basins, Turkey. Meteorological Applications, 24(1), 62-73.

Hao, Z., & AghaKouchak, A., 2013. Multivariate standardized drought index: a parametric multi-index model. Advances in Water Resources, 57, 12-18.

Hayes, M., Svoboda, M., Wall, N., & Widhalm, M., 2011. The Lincoln declaration on drought indices: Universal meteorological drought index recommended. Bulletin of the American Meteorological Society, 92(4), 485-488.

Hilario, F., de Guzman, R., Ortega, D., Hayman, P., & Alexander, B., 2009. El Niño Southern Oscillation in the Philippines: Impacts, forecasts, and risk management. Philippine Journal of Development, 36(1), 9.

Huffman, G. J., Bolvin, D. T., Braithwaite, D., Hsu, K., Joyce, R., Xie, P., & Yoo, S. H., 2020. NASA global precipitation measurement (GPM) integrated multi-satellite retrievals for GPM (IMERG). Algorithm Theoretical Basis Document (ATBD) Version 06.

Ji, L., & Peters, A. J., 2003. Assessing vegetation response to drought in the northern Great Plains using vegetation and drought indices. Remote Sensing of Environment, 87(1), 85-98.

Jordaan, A. J., Mlenga, D. H., & Mandebvu, B., 2019. Monitoring droughts in Eswatini: A spatiotemporal variability analysis using the Standard Precipitation Index. Jàmbá: Journal of Disaster Risk Studies, 11(1), 1-11.

Kogan, F. N., 1995. Application of vegetation index and brightness temperature for drought detection. Advances in Space Research, 15(11), 91-100.

Kogan, F., Salazar, L., & Roytman, L., 2012. Forecasting crop production using satellite-based vegetation health indices in Kansas, USA. International Journal of Remote Sensing, 33(9), 2798-2814.

Mo, K. C., 2011. Drought onset and recovery over the United States. Journal of Geophysical Research: Atmospheres, 116(D20).

National Disaster Risk Reduction and Management Council, 2019. SitRep No. 211 re Preparedness Measures and Effects of El Niño from https://ndrrmc.gov.ph/attachments/article/3676/SitRep_No_21_re_Prepareness_Measures_and_Effects_of_EL_Nino_Issued_on_21June2019_5Pm.pdf

Perez, G. J., Macapagal, M., Olivares, R., Macapagal, E. M., & Comiso, J. C., 2016. Forecasting and monitoring agricultural drought in the Philippines. International Archives of the Photogrammetry, Remote Sensing & Spatial

Information Sciences, 41.
Perez, G. J., Enricuso, O., Manauis, K., & Valete, M. A., 2022. Characterizing the drought development in the Philippines using multiple drought indices during the 2019 El Niño. ISPRS Annals of the Photogrammetry, Remote Sensing and Spatial Information Sciences, 3, 463-470
Sepulcre-Canto, G., Horion, S. M. A. F., Singleton, A., Carrao, H., & Vogt, J., 2012. Development of a Combined Drought Indicator to detect agricultural drought in Europe. Natural Hazards and Earth System Sciences, 12(11), 3519-3531.
Sutton, W. R., Srivastava, J. P., Rosegrant, M., Koo, J., & Robertson, R., 2019. Striking a Balance: Managing El Niño and La Niña in Lao PDR's Agriculture. World Bank.
Van Loon, A. F., 2015. Hydrological drought explained. Wiley Interdisciplinary Reviews: Water, 2(4), 359-392.
Wilhite, D. A., & Glantz, M. H., 1985. Understanding the drought phenomenon: The role of definitions. Water International, 10(3), 111-120.